J Therm Anal Calorim (2012) 110:715–723
DOI 10.1007/s10973-011-1887-9

Forward ion-exchange kinetics of heavy metal ions on the surface of carboxymethyl cellulose Sn(IV) phosphate composite nano-rod-like cation exchanger

Ali Mohammad · Inamuddin · Arshi Amin · Mu. Naushad · Gaber E. Eldesoky

Received: 5 July 2011 / Accepted: 25 August 2011 / Published online: 30 September 2011

Abstract The Nernst–Planck equations with some additional assumptions was used in this study to investigate the forward kinetics and ion-exchange mechanism of heavy metal ions viz. Ni^{2+}–H^+, Cu^{2+}–H^+, Mn^{2+}–H^+ and Zn^{2+}–H^+ on the surface of carboxymethyl cellulose Sn(IV) phosphate composite nano-rod-like cation-exchanger. It was observed that heavy metals' exchange processes were imparted by the particle diffusion-controlled phenomenon. Some physical parameters i.e., fractional attainment of equilibrium $U(\tau)$, self-diffusion coefficients (D_o), energy of activation (E_a), and entropy of activation (ΔS^*) were estimated. These investigations revealed that the equilibrium is attained faster at higher temperature probably because of availability of thermally enlarged matrix of carboxymethyl cellulose Sn(IV) phosphate composite nano-rod-like cation-exchange material. The physical parameters observed for this composite cation exchanger were also compared with other composite ion exchangers. The results showed that the ion-exchange phenomenon is more feasible on the surface of this composite cation exchanger as compared with the other ion exchangers which indicated the usefulness of this composite ion exchanger in various applications.

Keywords Carboxymethyl cellulose Sn(IV) phosphate · Organic–inorganic composite material · Cation-exchanger · Nano-rod, Ion-exchange kinetics

A. Mohammad (✉) · Inamuddin · A. Amin
Department of Applied Chemistry, Faculty of Engineering and Technology, Aligarh Muslim University, Aligarh 202002, India
e-mail: alimohammad08@gmail.com

Mu. Naushad · G. E. Eldesoky
Department of Chemistry, King Saud University, Building 5, Riyadh, Saudi Arabia

Abbreviations

$C_{19}H_{42}BrN$ (CTAB)	N-Cetyl-N,N,N-trimethyl ammonium bromide
C_5H_5N	Pyridine
DMW	Demineralize water
EDTA	Ethylene diamine tetra acetic acid
i.d.	Internal diameter

List of symbols

$U(\tau)$	Fractional attainment of equilibrium
D_o	Self diffusion coefficient
E_a	Energy of activation
ΔS^*	Entropy of activation
$\overline{D}_{H^+}$	Inter diffusion coefficient of counter ion H^+
$\overline{D}_{M^{2+}}$	Inter diffusion coefficient of counter ion M^{2+}
r_o	Particle radius
α	Mobility ratio
$Z_{H^+}/Z_{M^{2+}}$	Charge ratio
τ	A dimensionless time parameter
H^+	Hydrogen ion
M^{2+}	Metal ion
S	Slope
D	The ionic jump distance
k	The Boltzmann constant
R	The gas constant
h	Plank's constant
T	Temperature

Introduction

Organic–inorganic type composite materials is the latest study of interest in different laboratories for various applications [1–5], owing to their better thermal, chemical, and radiation stabilities compared with organic as well as

inorganic materials. Particularly, the applications of composite materials as ion exchangers have been of great interest in our laboratory in view of increasing environmental pollution concern [6–14]. In general, these composite ion-exchange materials have been developed by combination of insulating or conducting organic polymers as supporting materials and inorganic precipitates of polyvalent metal acid salt precursors by sol–gel method. Pristine inorganic ion exchangers and organic resins, for ion-exchange applications, have been of limited interest due to chemical and thermal stabilities, respectively. Furthermore, inorganic ion exchangers are reported to be not very much reproducible and granular thereby limiting their suitability for column operation. To overcome the limitation of pristine ion exchangers of organic and inorganic in nature, the organic polymer carboxymethyl cellulose was incorporated into the matrices of inorganic ion exchanger Sn(IV) phosphate leading to the formation of a new composite carboxymethyl cellulose Sn(IV) phosphate nano rod-like cation ion exchanger with better chemical, thermal, mechanical, granulometric, and ion-exchange properties [15]. Owing to the enhanced properties of composite materials, researchers have been motivated to have various applications of organic–inorganic composite ion exchangers in analytical and environmental chemistry [16–37]. New applications of composite materials have been explored in the fields of heterogeneous catalysis [38, 39], protective coatings [40], solid polymer electrolyte membrane fuel cells [41, 42], ion-selective membrane electrodes [37, 43], gas perm-selectivity [44, 45], ion transport [46, 47], and ion-exchange [48]. In most of these fields, information related to the ion-exchange kinetics and the mobility of counter ions in the lattice structure is needed. Kinetics studies envisage the three aspects of ion-exchange process, viz., the mechanism of ion exchange, rate-determining step, and the rate laws obeyed by the ion-exchange system. Moreover, the earlier approaches [49–52] of kinetic behavior were based on the old *Bt* criterion [53, 54], which is not very useful for a true ion-exchange (non-isotopic exchange) process because of the different effective diffusion coefficients and different mobilities [55] of the exchanging ions involved. The Nernst–Planck [56, 57] equations with some additional assumptions provide more appropriate values in obtaining the values of the various kinetic parameters precisely. Though many studies on the kinetics of ion exchange on organic and inorganic ion exchangers have been reported [58–61], relatively less information exists on the kinetics of exchange on composite ion-exchange materials. Hence, in this study carboxymethyl cellulose Sn(IV) phosphate nano-rod-like composite cation-exchanger was selected to evaluate the ion-exchange mechanism occurring over the surface of the cation exchanger. However, the synthesis, physico-chemical characterization, and thermodynamic study for the adsorption of pyridine of this composite cation exchanger have also been studied and results are published [15].

Experimental

Reagents and instruments

The main reagents, viz., stannic chloride, $SnCl_4{\cdot}5H_2O$ (95%), carboxymethyl cellulose sodium salt, *tri*-sodium orthophosphate dodecahydrate, $Na_3PO_4{\cdot}12H_2O$ (98%), and N-Cetyl-N,N,N-trimethyl ammonium bromide, $C_{19}H_{42}BrN$ (CTAB) (99%) used for the synthesis of the composite nano-rod-like cation-exchange material were obtained from Central Drug House (CDH) Pvt. Ltd., India. Pyridine, C_5H_5N (99%), nitric acid, HNO_3 (35%) and hydrochloric acid, HCl (35%) were obtained from E. Merck, India. Solutions for kinetic measurement were made using analytic reagent grade nitrate salts of Ni, Cu, Mn, and Zn (99%) obtained from Central Drug House Pvt. Ltd. India. The other reagents and chemicals used were of analytic reagent grade and used as received. A digital pH meter (Elico LI-10, India) to adjust the pH and a water bath incubator shaker for all equilibrium studies having a temperature variation of ±0.5 °C (MSW-275, India) were used.

Preparation of organic–inorganic composite cation-exchange material

Organic–inorganic composite cation exchanger carboxymethyl cellulose Sn(IV) phosphate composite nano-rod-like cation-exchange material was prepared as reported by Ali Mohammad et al. [15]. The procedure for the preparation is given below.

Preparation of reagent solutions

The solutions of 0.1 M stannic chloride ($SnCl_4{\cdot}5H_2O$) were prepared in 4 M HCl while 0.1 M *tri*-sodium orthophosphate ($Na_3PO_4{\cdot}12H_2O$), N-cetyl-N,N,N trimethyl ammonium bromide (CTAB), and carboxymethyl cellulose sodium salt (CMC) were prepared in demineralized water (DMW).

Preparation of carboxymethyl cellulose Sn(IV) phosphate composite nano-rod-like cation-exchange material

Sn(IV) phosphate was prepared by mixing 0.1 M stannic chloride solution with aqueous solution of 0.1 M *tri*-sodium orthophosphate in 1:2 (V/V) ratios at room temperature (25 ± 2 °C). White precipitate was obtained, when pH of the solution was adjusted to 1 by adding

aqueous ammonia/hydrochloric acid with constant stirring. 5 mL of CTAB was added to the precipitate of Sn(IV) phosphate and stirred for 10 min. Finally, 2 g of carboxymethyl cellulose sodium salt dissolved in 45 mL of DMW was added to the precipitate of Sn(IV) phosphate, stirred for 2 h, and finally kept for 24 h at room temperature (25 ± 2 °C) for digestion. The gels of Sn(IV) phosphate and carboxymethyl cellulose Sn(IV) phosphate composite cation exchanger were filtered off by suction; washed with DMW to remove excess acid. The washed gel was dried over P_4O_{10} at 40 °C in an oven. The dried product was washed again with acetone to remove impurities present in the material, and dried at 40 °C in an oven. The composite nano-rod-like cation exchanger carries fixed phosphate ionic groups which are converted into the form of H^+/counter ion by treating with 1 M HNO_3 for 24 h with occasional shaking and intermittently replacing the supernatant liquid with fresh acid 2–3 times. The excess acid was removed after several washings with DMW and finally dried at 50 °C. The composite nano-rod-like cation exchanger was cracked and the particle size of approximately 125 μm was obtained by sieving, and then stored in desiccator. The ion-exchange capacity was determined by standard column process. For this purpose, one gram (1 g) of the dry cation exchanger samples in the H^+-forms were taken into different glass columns having an internal diameter (i.d.) ~1 cm and fitted with glass wool support at the bottom. The bed length was approximately 1.5 cm long. 1 M $NaNO_3$ as eluent was used to elute the H^+ ions completely from the cation-exchange columns, maintaining a very slow flow rate (~0.5 mL min^{-1}). The effluents were titrated against a standard 0.1 M NaOH solution for estimating the total ions liberated in the solutions using phenolphthalein indicator and the ion-exchange capacities in meq dry g^{-1} are determined. The conditions of the preparation, the ion-exchange capacities, and the physical appearances of the inorganic and composite cation exchanger are given in Table 1. The ion-exchange capacity of composite nano-rod-like cation exchanger, carboxymethyl cellulose Sn(IV) phosphate, was found to be 2.13 meq dry g^{-1}, which is higher than inorganic counterpart Sn(IV) phosphate ion-exchange capacity of 1.2 meq dry g^{-1}. Thus, sample S-2 was selected for detailed kinetic studies.

Kinetic measurements

Composite cation-exchange particles of mean radius ~125 μm (50–70 mesh) in H^+ form were used to evaluate various kinetic parameters. The rate of exchange was determined by limited batch technique as follows:

A total of 20-mL fractions of the 0.03 M metal ion solutions (Ni, Cu, Mn, and Zn) were shaken with 200 mg of the cation exchanger in H^+-form in several stoppered conical flasks at desired temperatures [25, 35, 50, and 65 (±0.5) °C] for different time intervals (1.0, 2.0, 3.0, 4.0, and 25 min). The supernatant liquid was removed immediately and determinations were made as usual by ethylene diamine tetra acetic acid (EDTA) titrations [62]. Each set was repeated four times and the mean values were taken for calculation.

Results and discussions

Sol–gel method was employed to prepare carboxymethyl cellulose Sn(IV) phosphate composite cation exchanger (Table 1). Composite ion-exchange material possessed higher Na^+ ion-exchange capacity of 2.13 meq dry g^{-1} as compared to that of inorganic counterpart (1.20 meq dry g^{-1}). Composite cation-exchange particles of mean radius of ~125 μm (50–70 mesh) in H^+ form were used to study the kinetic behavior of heavy metal ions viz. Ni^{2+}–H^+, Cu^{2+}–H^+, Mn^{2+}–H^+ and Zn^{2+}–H^+. The rate-determining step in ion-exchange process may be either particle or film diffusion. Approximated Nernst–Planck equations are used to predict whether particle or film diffusion will be rate-controlling step under a given set of conditions. The infinite time of exchange is the time required to accomplish the equilibrium. Thus, the rate of exchange for metal ions becomes independent of time after this time interval. Figure 1 showed that equilibrium for Mg^{2+}–H^+ exchange at 35 °C was accomplished within 20 min. Similar behavior was also observed for Ni^{2+}–H^+, Cu^{2+}–H^+, Mn^{2+}–H^+, and Zn^{2+}–H^+ exchanges. Therefore, 20 min was assumed to be the infinite time of exchange for all exchange systems. A study of the concentration effect on the rate of exchange at 35 °C showed that the initial rate of exchange was proportional to the metal ion concentration, and τ versus time

Table 1 Conditions for the preparation of carboxymethyl cellulose Sn(IV) phosphate composite nano-rod-like cation exchanger

Samples	Mixing volume ratio (V/V)			Carboxymethyl cellulose sodium salt added/g	Color of beads obtained after drying	Na^+ ion exchange capacity/meq dry g^{-1}
	0.1 M $SnCl_4 \cdot 5H_2O$ in 4 M HCl	0.1 M $Na_3PO_4 \cdot 12H_2O$	pH			
1	1	2	1	–	White	1.20
2	1	2	1	2	White	2.13

(t) (t in min) plots are also straight lines passing through the origin at and above 0.03 M of metal ion concentration (data not shown), which confirms the particle diffusion-controlled phenomenon. Below the metal ion concentration of 0.03 M, film diffusion control phenomenon was more prominent.

Thus, kinetic measurements were achieved under particle diffusion-controlled ion-exchange phenomenon for the exchanges of Ni^{2+}–H^+, Cu^{2+}–H^+, Mn^{2+}–H^+, and Zn^{2+}–H^+. The kinetic results are expressed in terms of the fractional attainment of equilibrium, $U(\tau)$ with time according to the equation:

$$U(\tau) = \frac{\text{the amount of exchange at time } 't'}{\text{the amount of exchange at infinite time}} \quad (1)$$

Plots of $U(\tau)$ versus time (t) (t in min), for Ni^{2+}–H^+, Cu^{2+}–H^+, Mn^{2+}–H^+, and Zn^{2+}–H^+ exchanges (Fig. 2) showed that the fractional attainment of equilibrium was faster at a higher temperature suggesting that the mobility of the ions increased with an increase in temperature.

Each value of $U(\tau)$ will have a corresponding value of τ, a dimensionless time parameter. The numerical results for the calculation of τ can be expressed by Nernst–Planck explicit approximation [63–65]:

$$U(\tau) = \{1 - \exp[\pi^2(f_1(\alpha)\tau + f_2(\alpha)\tau^2 + f_3(\alpha)\tau^3)]\}^{1/2} \quad (2)$$

where τ is the half time of exchange $= \overline{D}_{H^+}t/r_o^2$, α is the mobility ratio $= \overline{D}_{H^+}/\overline{D}_{M^{2+}}$, r_o is the particle radius, $\overline{D}_{H^+}$ and $\overline{D}_{M^{2+}}$ are the inter diffusion coefficients of counter ions H^+ and M^{2+}, respectively, in the exchanger phase. The three functions $f_1(\alpha)$, $f_2(\alpha)$, and $f_3(\alpha)$ depend on the mobility ratio (α) and the charge ratio ($Z_{H^+}/Z_{M^{2+}}$) of the exchanging ions. Thus, they have different expressions as given below. When the exchanger is taken in the H^+-form and the exchanging ion is M^{2+}, for $1 \leq \alpha \leq 20$, as in the present case, the three functions have the values:

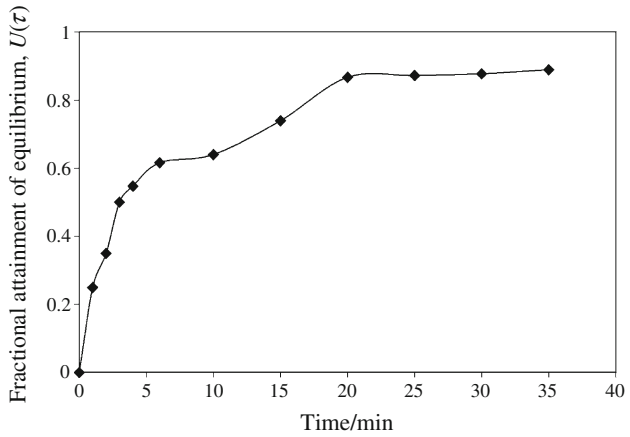

Fig. 1 A plot of $U(\tau)$ versus t (time) for M^{2+}–H^+ exchanges at 35 °C on carboxymethyl cellulose Sn(IV) phosphate composite nano-rod-like cation exchanger for the determination of infinite time

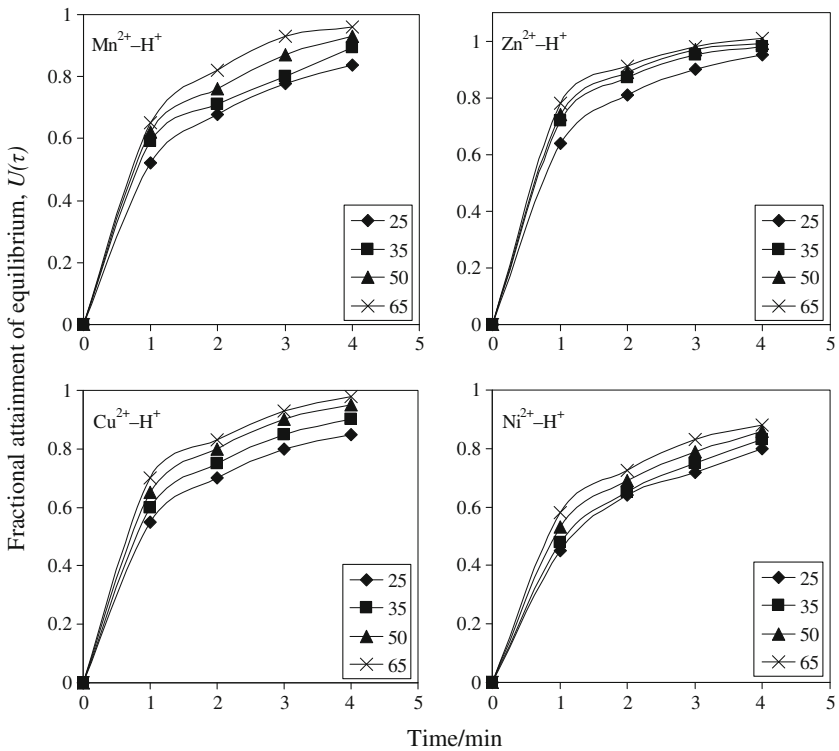

Fig. 2 Plots of $U(\tau)$ versus t (time) for Ni^{2+}–H^+, Cu^{2+}–H^+, Mn^{2+}–H^+, and Zn^{2+}–H^+ exchanges at different temperatures on carboxymethyl cellulose Sn(IV) phosphate composite nano-rod-like cation exchanger

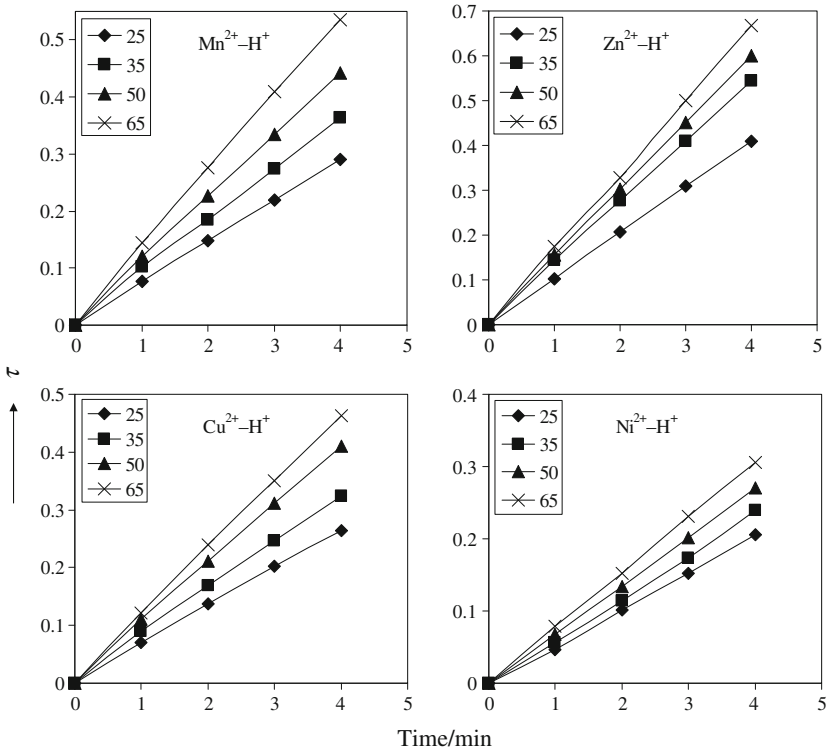

Fig. 3 Plots of τ versus t (time) for Ni^{2+}–H^+, Cu^{2+}–H^+, Mn^{2+}–H^+, and Zn^{2+}–H^+ exchanges at different temperatures on carboxymethyl cellulose Sn(IV) phosphate composite nano-rod-like cation exchanger

Table 2 Slopes of various τ versus time (t) plots on carboxymethyl cellulose Sn(IV) phosphate composite nano-rod-like cation exchanger at different temperatures

Migrating ions	$S/s^{-1} \times 10^2$			
	Temperature			
	25 °C	35 °C	50 °C	65 °C
Cu(II)	6.6	8.2	10.3	11.6
Ni(II)	5.0	5.8	6.7	7.6
Zn(II)	10.2	13.6	15.0	16.6
Mn(II)	7.3	9.1	11.1	13.5

$$f_1(\alpha) = -\frac{1}{0.64 + 0.36\alpha^{0.668}}$$

$$f_2(\alpha) = -\frac{1}{0.96 - 2.0\alpha^{0.4635}}$$

$$f_3(\alpha) = -\frac{1}{0.27 + 0.09\alpha^{1.140}}$$

The value of τ was obtained on solving Eq. 2 using a computer. The plots of τ versus time (t) at four different temperatures for Ni^{2+}–H^+, Cu^{2+}–H^+, Mn^{2+}–H^+, and Zn^{2+}–H^+ exchanges are shown in Fig. 3 are straight lines passing through the origin, confirming the particle diffusion control phenomenon for M^{2+}–H^+ exchanges at a metal ion concentration of 0.03 M. It is obvious that the particle diffusion-controlled exchange is more rapid when the counter ion which is initially in the ion exchanger is the faster one, while for the film diffusion-controlled exchange, the counter ion which is preferred by the ion exchanger is taken up at the higher rate and released at the lower rate.

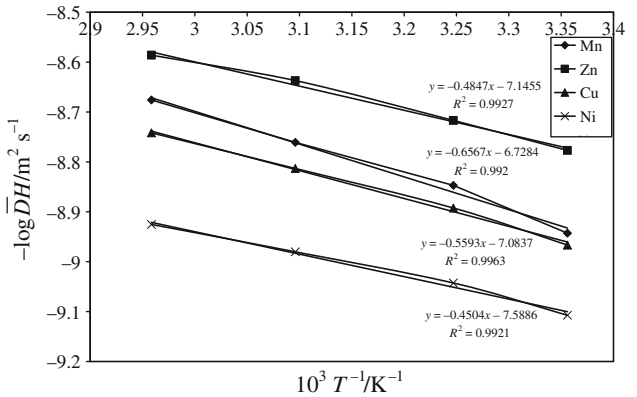

Fig. 4 Plots of $-\log \overline{D}_{H^+}$ versus 10^3 T^{-1}/K^{-1} for Ni^{2+}–H^+, Cu^{2+}–H^+, Mn^{2+}–H^+, and Zn^{2+}–H^+ on exchanges on carboxymethyl cellulose Sn(IV) phosphate composite nano-rod-like cation exchanger

The slopes (S values) of various τ versus time (t) plots are given in Table 2. The S values are related to $\overline{D}_{H^+}$ as follows:

$$S = \overline{D}_{H^+} / r_o^2 \quad (3)$$

The values of $-\log \overline{D}_{H^+}$ obtained by using Eq. 3 plotted against $1/T$ are straight lines as shown in Fig. 4, thus verifying the validity of the Arrhenius relation:

Table 3 Values of D_o, E_a, and ΔS^* for the exchange of H^+ ions with some metal ions on carboxymethyl cellulose Sn(IV) phosphate composite nano-rod-like composite cation-exchange material

Metal ion exchange with H(I)	10^9 Ionic mobility/m^2 V^{-1} s^{-1}	10^2 Ionic radii/nm	10^8 D_o/m^2 s^{-1}	10^2 E_a/kJ mol^{-1}	ΔS^*/J K^{-1} mol^{-1}
Cu(II)	57	7.0	8.2604	55.9	−0.7508
Ni(II)	52	7.8	2.5823	45.04	−1.2557
Zn(II)	56	8.3	7.1614	48.4	−0.8128
Mn(II)	55	9.1	0.18707	65.6	−0.3958

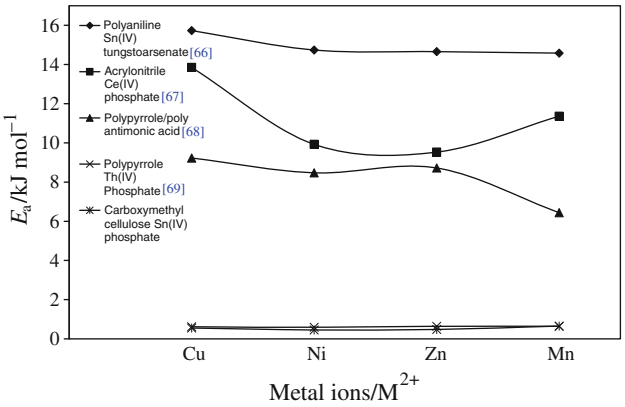

Fig. 5 Plots of activation energy (E_a) of Ni^{2+}–H^+, Cu^{2+}–H^+, Mn^{2+}–H^+, Zn^{2+}–H^+ for various composite cation exchangers

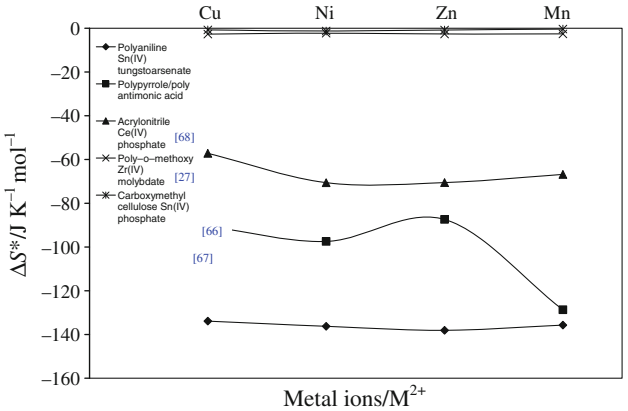

Fig. 6 Plots of entropy of activation (ΔS^*) of Ni^{2+}–H^+, Cu^{2+}–H^+, Mn^{2+}–H^+, Zn^{2+}–H^+ for various composite cation exchangers

$$\overline{D}_{H^+} = D_o \exp(-E_a/RT) \quad (4)$$

D_o is obtained by extrapolating these lines and using the intercepts at the origin. The activation energy (E_a) is then calculated with the help of the Eq. 4, putting the value of $\overline{D}_{H^+}$ at 273 K. The entropy of activation (ΔS^*) was then calculated by substituting D_o in Eq. 5.

$$D_o = 2.72 d^2 (kT/h) \exp(\Delta S^*/R) \quad (5)$$

where d is the ionic jump distance taken as 5×10^{-10} m, k is the Boltzmann constant, R is the gas constant, h is Plank's constant, and T is taken as 273 K. The values of the diffusion coefficient (D_o), energy of activation (E_a), and entropy of activation (ΔS^*) thus obtained are summarized in Table 3.

No definite relation between the ionic radii and mobility of metal ions with activation energy and entropy of activation was observed. However, the positive values of activation energy indicated that the minimum energy is required to facilitate the forward (M^{2+}–H^+) ion-exchange process. Negative values of the entropy of activation (ΔS^*) suggest a greater degree of order achieved during the forward ion-exchange (M^{2+}–H^+) process. A comparison of forward ion-exchange kinetics behavior of this composite cation exchanger with those of various other composite cation exchangers is given in Figs. 5 and 6. It was observed that the proposed composite cation exchanger possessed lower activation energy to facilitate the ion-exchange process (Fig. 5). Lower negative values of ΔS^* indicated that the randomness of this composite cation exchanger is much higher than other composite materials (Fig. 6). Thus, the ion exchange process is spontaneous in the forward direction than the other composite cation-exchange materials.

Conclusions

The ion-exchange kinetic study showed that equilibrium is attained faster at a higher temperature which may be due to the higher diffusion rate of ions through the thermally enlarged interstitial positions of the ion-exchange matrix. The kinetic-exchange in the forward direction (M^{2+}–H^+) for this composite cation exchanger is being governed by the particle diffusion-controlled phenomenon which is faster than the film diffusion-controlled phenomenon. Activation energy is calculated by using verified and validated Arrhenius equation which showed that lower energy is required to accomplish the ion exchange process. The negative values of (ΔS^*) indicate that the ion-exchange process (M^{2+}–H^+) is more feasible under given set of conditions on this composite cation-exchange material.

Acknowledgements The authors are thankful to the Department of Applied Chemistry, Z. H. College of Engineering and Technology, A.M.U. (Aligarh) for providing research facilities and the Deanship of Scientific Research at King Saud University for funding the study through the research group project No RGP-VPP-130.

References

1. Zhang J, Li B, Wang Z, Cheng G, Dong S. Functionalized inorganic–organic composite material derivated by sol–gel for construction of mediated amperometric hydrogen peroxide biosensor. Anal Chim Acta. 1999;388:71–8.
2. Lakshminarayana G, Nogami M, Kityk IV. Synthesis and characterization of anhydrous proton conducting inorganic-organic composite membranes for medium temperature proton exchange membrane fuel cells (PEMFCs). Energy. 2010;35:5260–8.
3. Kameda T, Takeuchi H, Yoshioka T. Hybrid inorganic/organic composites of Mg–Al layered double hydroxides intercalated with citrate, malate, and tartrate prepared by co-precipitation. Mater Res Bull. 2009;44:840–5.
4. Smaihi M, Jermoumi T, Marignan J, Noble RD. Organic-inorganic gas separation membranes: preparation and characterization. J Membr Sci. 1996;116:211–20.
5. Fujiwara M, Sakamoto A, Shiokawa K, Patra AK, Bhaumik A. Mesoporous MFI zeolite material from silica–alumina/epoxy-resin composite material and its catalytic activity. Microporous Mesoporous Mater. 2011;142:381–8.
6. Nabi SA, Naushad Mu, Inamuddin. Synthesis, characterization and analytical applications of a new highly thermally and chemically stable semi-crystalline inorganic ion-exchanger: Zr(IV) tungstomolybdate. J Hazard Mater. 2007;142:404–11.
7. Khan AA, Inamuddin, Alam MM. Preparation, characterization and analytical applications of a new and novel electrically conducting fibrous type polymeric-inorganic composite material: polypyrrole Th(IV) phosphate used as a cation-exchanger and Pb(II) ion-selective membrane electrode. Mater Res Bull. 2005;40:289–305.
8. Inamuddin, Khan SA, Siddiqui WA, Khan AA. Synthesis, characterization and ion-exchange properties of a new and novel 'organic-inorganic' hybrid cation-exchanger: Nylon-6,6, Zr(IV) phosphate. Talanta. 2007;71:841–7.
9. Khan AA, Inamuddin. Preparation, physico-chemical characterization, analytical applications and electrical conductivity measurement studies of an 'organic-inorganic' composite cation-exchanger: polyaniline Sn(IV) phosphate. React Funct Polym. 2006;66:1649–63.
10. Siddiqui WA, Khan SA, Inamuddin. Synthesis, characterization and ion-exchange properties of a new and novel 'organic–inorganic' hybrid cation-exchanger: poly(methyl Methacrylate) Zr(IV) phosphate. Colloids Surf A Physicochem Eng Asp. 2007;295:193–7.
11. Khan AA, Khan A, Inamuddin. Synthesis and characterization of a new nanocomposite cation-exchanger poly-o-toluidine Th(IV) phosphate and its application in the fabrication of ion-selective membrane electrode. Talanta. 2007;72:699–710.
12. Inamuddin, Ismail YA. Synthesis and characterization of poly-o-methoxyaniline Zr(1 V) molybdate Cd(II) selective composite cation-exchanger. Desalination. 2010;250:523–9.
13. Alam Z, Inamuddin, Nabi SA. Synthesis and characterization of a thermally stable strong acidic Cd(II) selective composite cation-exchanger: polyaniline Ce(IV) molybdate. Desalination. 2010;250:515–22.
14. Mohammad A, Inamuddin, Amin A. Nano-composite cation-exchanger polyvinyl alcohol Sn(IV) tungstate: preparation, characterization, thermodynamic study and its analytical application for the adsorption of aniline. J Therm Anal Calorim. (2011). doi:10.1007/s10973-011-1534-5.
15. Mohammad A, Inamuddin, Amin A. Surfactant assisted preparation, characterization and thermodynamic study of pyridine adsorption on carboxymethyl cellulose Sn(IV) phosphate composite nano-rod like cation exchanger. J Therm Anal Calorim. doi:10.1007/s10973-011-1548-z.
16. Mojumdar SC, Raki L. Preparation and properties of calcium silicate hydrate-poly (vinyl alcohol) nanocomposite materials. J Therm Anal Calorim. 2005;82:89–95.
17. Mukherjee GS. Calorimetric characterization of membrane materials based on polyvinyl alcohol. J Therm Anal Calorim. 2009;96(1):21–5.
18. Bittencourt PRS, Santos GLD, Pineda EAG. Hechenleitner. Studies on the thermal stability and film irradiation effect of poly (vinyl alcohol)/Kraft lignin blends. J Therm Anal Calorim. 2005;79:371–4.
19. Cuiying L, Wei Z, Bo Z, Mei L, Canhui L. Preparation, characterization and thermal behaviour of poly(vinyl alcohol)/organic montmorillonite nanocomposites through solid-state shear pan-milling. J Therm Anal Calorim. 2011;103(1):205–12.
20. Vlase G, Vlase T, Doca N, Perta M, Ilia G, Plesu N. Thermal behaviour of a sol-gel system containing aniline and organic phosphonates. J Therm Anal Calorim. 2009;97:473–8.
21. Shady SA. Selectivity of cesium from fission radionuclides using resorcinol formaldehyde and zirconyl-molybdopyrophosphate as ion-exchangers. J Hazard Mater. 2009;167:947–52.
22. Nilchi A, Naushad Mu, Al-Othman ZA. Development, characterization and ion exchange thermodynamics for a new crystalline composite cation exchange material: application for the removal of Pb^{2+} ion from a standard sample (Rompin Hematite). J Inorg Organomet Polym. doi:10.1007/s10904-011-9491-9.
23. Zhang H, Pang JH, Wang D, Li A, Li X, Jiang Z. Sulfonated poly(arylene ether nitrile ketone) and its composite with phosphotungstic acid as materials for proton exchange membranes. J Membr Sci. 2005;264:56–64.
24. Al-Othman ZA, Inamuddin, Naushad Mu. Forward (M^{2+}–H^{+}) and reverse (H^{+}–M^{2+}) ion exchange kinetics of the heavy metals on polyaniline Ce(IV) molybdate: a simple practical approach for the determination of regeneration and separation capability of ion exchanger. Chem Eng J. 2011;171:456–63.
25. Al-Othman ZA, Inamuddin, Naushad Mu. Adsorption thermodynamics of trichloroacetic acid herbicide on polypyrrole Th(IV) phosphate composite cation-exchanger. Chem Eng J. 2011;169:38–42.
26. Varshney KG, Rafiquee MZA, Somya A, Drabik M. Synthesis and characterization of a Hg(II) selective n-butyl acetate cerium(IV) phosphate as a new intercalated fibrous ion exchanger: effect of surfactants on the adsorption behaviour. Indian J Chem Sec A Inorg Phys Theor Anal Chem. 2006;45:1856–60.
27. Al-Othman ZA, Inamuddin, Naushad Mu. Determination of ion-exchange kinetic parameters for the poly-o-methoxyaniline Zr(IV) molybdate composite cation-exchanger. Chem Eng J. 2011;166:639–45.
28. Nabi SA, Shalla AH. Synthesis, characterization and analytical application of hybrid; acrylamide zirconium (IV) arsenate a cation exchanger, effect of dielectric constant on distribution coefficient of metal ions. J Hazard Mater. 2009;163:657–64.
29. Varshney KG, Tayal N. Polystyrene thorium(IV) phosphate as a new crystalline and cadmium selective fibrous ion exchanger. Synthesis characterization and analytical applications. Langmuir 2001;2589–2593.
30. Moon JK, Kim KW, Jung CH, Shul YG, Lee EH. Preparation of organic-inorganic composite adsorbent beads for removal of

radionuclides and heavy metal ions. J Radioanal Nucl Chem. 2000;246:299–307.
31. Varshney KG, Agrawal A, Mojumdar SC. Pectin based cerium (IV) and thorium (IV) phosphates as novel hybrid fibrous ion exchangers synthesis, characterization and thermal behaviour. J Therm Anal Calorim. 2005;81:183–9.
32. Nabi SA, Bushra R, Al-Othman ZA, Naushad Mu. Synthesis, characterization and analytical applications of a new composite cation exchange material Acetonitrile stannic(IV) selenite: adsorption behavior of toxic metal ions in nonionic surfactant medium. Sep Sci Technol. 2011;46:847–57.
33. Gupta AP, Agarwal H, Ikram S. Studies on new composite material polyaniline Zirconium (IV) tungstophosphate; Th(IV) selective cation exchanger. J Indian Chem Soc. 2003;80:57–9.
34. Shaw MJ, Nesterenko PN, Dicinoski GW, Haddad PR. Selectivity behaviour of a bonded phosphonate–carboxylate polymeric ion exchanger for metal cations with varying eluent compositions. J Chromatogr A. 2003;997:3–11.
35. Koseoglu TS, Kir E, Ozkorucuklu SP, Karamizrak E. Preparation and characterization of P2FAn/PVDF composite cation-exchange membranes for the removal of Cr(III) and Cu(II) by Donnan dialysis. React Funct Polym. 2010;70:900–7.
36. Sundaram CS, Meenakshi S. Fluoride sorption using organic–inorganic hybrid type ion exchangers. J Colloids Interface Sci. 2009;333:58–62.
37. Khan AA, Inamuddin. Applications of Hg(II) sensitive polyaniline Sn(IV) phosphate composite cation-exchange material in determination of Hg^{2+} from aqueous solutions and in making ion-selective membrane electrode. Sens Actuat B Chem. 2006;120:10–8.
38. Li H, Zheng Z, Cao M, Cao R. Stable gold nanoparticle encapsulated in silica-dendrimers organic–inorganic hybrid composite as recyclable catalyst for oxidation of alcohol. Microporous Mesoporous Mater. 2010;136:42–9.
39. Dallmann K, Buffon R. Sol–gel derived hybrid materials as heterogeneous catalysts for the epoxidation of olefins. Catal Commun. 2000;1:9–13.
40. Chaudhari S, Sainkar SR, Patil PP. Corrosion protective poly(o-ethoxyaniline) coatings on copper. Electrochim Acta. 2007;53:927–33.
41. Zhang Y, Zhang HM, Bi C, Zhu XB. An inorganic/organic self-humidifying composite membranes for proton exchange membrane fuel cell application. Electrochim Acta. 2008;53:4096–103.
42. Malers JL, Sweikart MA, Horan JL, Turner JA, Herring AM. Studies of heteropoly acid/polyvinylidenedifluoride–hexafluoroproylene composite membranes and implication for the use of heteropoly acids as the proton conducting component in a fuel cell membrane. J Power Sources. 2007;172:83–8.
43. Nabi SA, Alam Z, Inamuddin. A cadmium ion-selective membrane electrode based on strong acidic organic inorganic composite cation-exchanger: polyaniline Ce(IV) molybdate. Sens Transd J (S & T e-Digest). 2008;92:87–9.
44. Guizard C, Bac A, Barboiu M, Hovnanian N. Hybrid organic-inorganic membranes with specific transport properties: applications in separation and sensors technologies. Sep Purif Technol. 2001;25:167–80.
45. Iwata M, Adachi T, Tonidokoro M. Hybrid sol–gel membranes of polyacrylonitrile–tetraethoxysilane composites for gas perm selectivity. J Appl Polym Sci. 2003;88:1752–9.
46. Lacan P, Guizard C, Gall PL. Facilitated transport of ions through fixed-site carrier membranes derived from hybrid organic-inorganic materials. J Membr Sci. 1995;100:99–109.
47. Kumar M, Tripathi BP, Shahi VK. Ionic transport phenomenon across sol–gel derived organic–inorganic composite mono-valent cation selective membranes. J Membr Sci. 2009;340:52–61.
48. Nilchi A, Khanchi A, Atashi H, Bagheri A, Nematollahi L. The application and properties of composite sorbents of inorganic ion exchangers and polyacrylonitrile binding matrix. J Hazard Mater A. 2006;137:1271–6.
49. Clearfield A, Medina AS. On the mechanism of ion exchange in crystalline zirconium phosphates—III: the dehydration behavior of sodium ion exchanged phases of α-zirconium phosphate. J Inorg Nucl Chem. 1970;32:2775–80.
50. Alberti G, Bertrami R, Caseola M, Costantino U, Gupta JP. Crystalline insoluble acid salts of tetravalent metals—XXI ion exchange mechanism of alkaline earth metal: ions on crystalline $ZrHNa(PO_4)_2{\cdot}5H_2O$. J Inorg Nucl Chem. 1976;38:843–8.
51. Saraswat IP, Srivastava SK, Sharma AK. Kinetics of ion exchange of some complex cations on chromium ferrocyanide gel. Can J Chem. 1979;57:1214–7.
52. Singh NJ, Mathew J, Tandon SN. Kinetics of ion exchange. A radiochemical study of rubidium(1+)-hydrogen(1+) and silver(1+)-hydrogen(1+) exchange on zirconium arsenophosphate. J Phys Chem. 1980;84:21.
53. Boyd GE, Adamson AW, Myers LS. The exchange adsorption of ions from aqueous solutions by organic zeolites. II. Kinetics. J Am Chem Soc. 1947;69:2836–48.
54. Reichenberg D. Properties of ion-exchange resins in relation to their structure. III. Kinetics of exchange. J Am Chem Soc. 1953;75:589–97.
55. Helfferich F. Ion exchange. McGraw-Hill: New York; 1962 (Chapter 6).
56. Nernst WH. Die elektromotorische wirksamkeit der ionen. Z Phys Chem. 1889;4:129–81.
57. Planck M. Über die erregung von elektricität und wärme in elektrolyten. Ann Physik und Chemie Neue Folge. 1890;39:161–86.
58. Sari A, Çitak D, Tuzen M. Equilibrium, thermodynamic and kinetic studies on adsorption of Sb(III) from aqueous solution using low-cost natural diatomite. Chem Eng J 2010;162:521–527.
59. Varshney KG, Khan AA, Rani S. Forward and reversible ion exchange kinetics for Na^+–H^+ and K^+–H^+ exchanges on crystalline antimony (V) silicate cation exchanger. Colloids Surf A Physicochem Eng Asp. 1987;25:131–7.
60. Varshney KG, Gupta A, Singhal KC. Synthetic, analytical and kinetic studies on a crystalline and thermally stable phase of antimony (V) arsenosilicate cation exchanger. Colloids Surf A Physicochem Eng Asp. 1994;82:37–48.
61. Gupta AP, Varshney PK. Investigation of some kinetic parameters for M^{2+}–H^+ exchanges on zirconium(IV) tungstophosphate—a cation exchanger. React Polym. 1997;32:67–74.
62. Reilley CN, Schmidt RW, Sadek FS. Chelon approach (I) survey of theory and application. J Chem Educ. 1959;36:555–65.
63. Kodama S, Fukui K, Mazume A. Relation of space velocity and space time yield. Ind Eng Chem. 1953;45:1644–8.
64. Helfferich F, Plesset MS. Ion exchange kinetics: a nonlinear diffusion problem. J Chem Phys. 1958;28:418–24.
65. Plesset MS, Helfferich F, Franklin JN. Ion exchange kinetics: a nonlinear diffusion problem. II. Particle diffusion controlled exchange of univalent and bivalent ions. J Chem Phys. 1958;29:1064–9.
66. Khan AA, Alam MM, Mohammad F. Ion-exchange kinetics and electrical conductivity studies of polyaniline Sn(IV)tungstoarsenate; $(SnO_2)(WO_3)(As_2O_5)_4(C_6H_5NH_2)_2.nH_2O$: a new semi-crystalline 'polymeric_/inorganic' composite cation-exchange material. Electrochim Acta. 2003;48:2463–72.
67. Varshney KG, Tayal N. Ion exchange of alkaline earth and transition metal ions on fibrous acrylonitrile based cerium (IV) phosphate—a kinetic study. Colloids Surf A Physicochem Eng Asp. 2000;162:49–53.

68. Khan AA, Alam MM, Inamuddin, Mohammad F. Electrical conductivity and ion-exchange kinetic studies of a crystalline type 'organic-inorganic' cation-exchange material: polypyrrole/poly-antimonic acid composite system, (Sb_2O_5) $(–C_4H_2$ NH–)·nH_2O. J Electroanal Chem. 2004;572:67–78.

69. Khan AA, Inamuddin. Cation-exchange kinetics and electrical conductivity measurement studies of an electrically conducting 'organic-inorganic' composite cation-exchanger: polypyrrole Th(IV) phosphate. J Appl Polym Sci. 2007;105:2806–15.